American Mineralogist, Volume 72, pages 979–983, 1987

Neutron-diffraction study of bertrandite

JAMES W. DOWNS
Department of Geology and Mineralogy, The Ohio State University, Columbus, Ohio 43210, U.S.A.
F. K. ROSS
Research Reactor Facility, University of Missouri, Columbia, Missouri 65211, U.S.A.

ABSTRACT

The crystal structure of bertrandite [$Be_4Si_2O_7(OH)_2$] is refined from room-temperature single-crystal neutron-diffraction data to $R(F^2)$ of 4.81% from 741 observations. Extinction is found to be significantly anisotropic. The refined H positions reveal a zigzag chain of weak H bonds with (H···O) distances of 2.33 and 2.39 Å.

INTRODUCTION

Bertrandite [$Be_4Si_2O_7(OH)_2$] is one of the 20 known phases of the system BeO-Al_2O_3-SiO_2-H_2O (BASH) and is the principal ore of beryllium (Petkof, 1976). The crystal structure of bertrandite was originally solved by Solov'eva and Belov (1965) and has recently been refined by X-ray diffraction data taken at several pressures by Hazen and Au (1986).

The principal objective of the present study was to locate accurately the H positions in order to examine the possibility of H bonding in bertrandite. Such bonding may be significant in understanding the stabillty of hydrous vs. anyhydrous minerals in the BASH system.

DATA COLLECTION AND REDUCTION

The crystal of bertrandite used for this study is from Beryl Mountain, New Hampshire, and was obtained from Carl Francis at the Harvard University Mineralogical Museum (HMM no. 103454). Most of the pertinent crystallographic information is given in Table 1. The crystal is an optically clear plate with (001) and (00$\bar{1}$) as the dominant forms. A microprobe analysis shows Si to be the only detectable cation. The water content of the sample was not determined.

Neutron-diffraction data were collected at the University of Missouri Research Reactor Facility (MURR) using diffractometer 2XE. An orientation matrix was obtained from the angles of 20 automatically centered reflections. Although intensities from each octant of reciprocal space were examined, only those that were found to be significantly above background during a prescan were fully step-scanned. The neutron wavelength of 1.075 Å was obtained from the 220 reflection of a Cu monochromator crystal, and scattered neutrons were detected with a BF_3 detector. Three standard reflections were measured every 75 observations, and no significant variation was observed in their intensities.

Peak profiles were reduced to integrated intensities using the algorithm of Lehmann and Larsen (1974) as coded in the interactive profile-analysis program INTEGRSTP written by Larry Finger. The linear absorption coefficient given in Table 1 was calculated using coherent and incoherent absorption cross-section values taken from Bacon (1975). The absorption cross section for H was taken to be 34.19×10^{-28} m^2 of which 34 (10^{-28} m^2) is due to incoherent neutron scattering for a H-bonded H atom. These intensities were then corrected for Lorentz and absorption effects. The rejection of discordant reflections and data averaging were completed using program SORTAV (Robert H. Blessing, pers. comm.). Anticipating the refinement of anisotropic extinction parameters, data were averaged in Laue group $\bar{1}$ as well as group *mmm*. Although refinements using only the $\bar{1}$ averaged data are reported here, statistics from both sorts are included in Table 1.

LEAST-SQUARES REFINEMENTS

Crystal-structure refinements were completed using full-matrix least-squares procedures as coded in program LINEX (Coppens, 1975), a modified version of ORFLS (Busing et al., 1962), using values for the coherent neutron-scattering lengths from Koester (1977). Initial refinements were completed without H atoms in the model using the atomic coordinates of Solov'eva and Belov (1965). H positions were included in the refinement after their initial location using difference Fourier techniques.

In accordance with the results of previous studies, Be and Si were assumed to be perfectly ordered; therefore, no site-population refinements were completed. Extinction was modeled within the limitation of the Darwin-Zachariasen-Hamilton transfer equations, using the formalism of Becker and Coppens (1974a, 1974b, 1975), and was assumed to be mosaic spread dominated (type I) with a Lorentzian distribution function. The structure-factor model included a scale factor, positional parameters, anisotropic thermal parameters for all atoms, and extinction parameters as variables. All refinements were based on $|F|^2$ using data averaged in Laue group $\bar{1}$. The weight for each observation was given by 1/var, where var is the variance in the averaged $|F|^2$ given by counting statistics alone. No ignorance factor was included in the weighting scheme.

Extinction can be severe for silicate minerals and is probably the most serious obstacle to be surmounted in obtaining truly accurate results from single-crystal neutron or X-ray diffraction data. Luckily, positional parameters are usually little affected by the details of the extinction model (Becker, 1977); however, vibrational

0003–004X/87/0910–0979$02.00

TABLE 1. Crystallographic data

Space group	$Cmc2_1$	
Unit-cell dimensions*		
a (Å)	8.7135 (4)	
b	15.268 (1)	
c	4.5683 (3)	
Crystal dimensions (mm)	2.5 × 2.0 × 1.0	
Crystal volume (mm³)	5.01	
Absorption coefficient (cm^{-1})	0.926	
Temperature (K)	295 (2)	
Range of sin θ/λ ($Å^{-1}$)	0.114–0.686	
Step-scan mode	θ–2θ	
Step size (°2θ)	0.05	
Steps per scan	40–60	
No. of reflections	1579	
Range of transmission factors	0.84–0.91	
Data averaging:		
Laue group	*mmm*	$\bar{1}$
No. reflections rejected	168	94
$R = \Sigma F_o^2 - \langle F_o^2 \rangle / \Sigma F_o^2$	0.0319	0.0278
R for all observations	0.0480	0.0420
No. obs. after averaging	363	741
No. unmeasured obs. with sin $\theta/\lambda < 0.686$	118	799

* From Hazen and Au (1986).

parameters can be severely affected (Downs et al., 1985). Extinction is generally anisotropic and is described by a second-rank tensor (Coppens and Hamilton, 1970), even though one could imagine such a property to be of higher rank. Anisotropic extinction can cause the integrated intensities of otherwise symmetry-equivalent reflections to be nonequivalent. Since it is assumed that anisotropic extinction is a second-rank property, Friedel pairs should be equivalent. It is therefore common practice when refining anisotropic extinction to use only data averaged in Laue group $\bar{1}$, regardless of the crystal symmetry. The figures of merit for refinements including isotropic and anisotropic extinction are given in Table 2.

The anisotropic extinction ellipsoid is of the form proposed by Thornley and Nelmes (1974). The hypothesis that extinction was isotropic was tested using the R-factor ratio test of Hamilton (1965). The R-factor ratio based on $R_{\text{isotropic}}/R_{\text{anisotropic}} = 1.158$ yields $R_{5,561,0.005} = 1.013$, which means that we may reject the hypothesis that extinction is isotropic at the 0.005 level. Extinction therefore appears to be significantly anisotropic. The refined elements of the extinction tensor, its eigenvalues, and the angles

TABLE 2. Figures of merit from least-squares refinements

	Isotropic extinction	Anisotropic extinction
N_o = number of observations	741	741
N_v = number of variables	85	90
$\epsilon = \Sigma w(\lvert F_o \rvert^2 - k^2 \lvert F_c \rvert^2)^2$	1765	1280
$R(F) = \Sigma \lvert \lvert F_o \rvert - k \lvert F_c \rvert \rvert / \Sigma \lvert F_o \rvert$	0.0385	0.0339
$R(F^2) = (\Sigma \lvert \lvert F \rvert^2 - k^2 \lvert F_c \rvert^2 \rvert / \Sigma \lvert F_o \rvert^4)^{1/2}$	0.0586	0.0481
$R_w(F^2) = (\epsilon / \Sigma w \lvert F_o \rvert^4)^{1/2}$	0.0799	0.0680
$S = [\epsilon/(N_o - N_v)]^{1/2}$	1.640	1.402
Scale factor (k)	8.21 (5)	8.35 (4)
Smallest extinction factor (y)	0.60	0.57
$F_c^2 = yk^2F_k^2$		

TABLE 3. Anisotropic extinction parameters and ellipsoid

			Angle (°) with respect to		
		η''	a	b	c
Y_{11}	59 (6)				
Y_{22}	8 (2)				
Y_{33}	55 (8)	33 (2)	137	99	48
Y_{12}	17 (3)	2 (1)	63	148	74
Y_{13}	−42 (6)	15 (1)	58	60	47
Y_{23}	−4 (2)				

that the eigenvectors make with the direct-basis vectors are given in Table 3. For type-I anisotropic extinction, the value for the extinction correction of a given reflection depends upon **D**, the vector perpendicular to the diffraction plane. Any symmetry-equivalent reflections that share this vector will receive the same extinction correction. The eigenvalues are given in seconds of arc and represent the mosaic spread for crystal rotation about a **D** vector along the corresponding eigenvector.

Atomic positions, apparent vibrational ellipsoids, and selected interatomic distances obtained from the anisotropic extinction refinement are listed in Tables 4–7. The observed and calculated structure-factor moduli for each observation are given in Table 8.[1]

DISCUSSION

The atomic positions and interatomic distances obtained from this study are within 3 estimated standard deviations of those reported by Hazen and Au (1986). Some of the interatomic distances reported here differ substantially from those of Solov'eva and Belov (1965), who, in the first structure refinement of bertrandite, reported Be–O distances of 1.58 and 1.78 Å that are outside of the range generally expected for this bond (Downs and Gibbs, 1981).

For bertrandite, the principal advantage of neutron diffraction over X-ray diffraction is that, because of the large negative neutron-scattering length of H, the H positions

[1] To obtain a copy of Table 8, order Document Am-87-353 from the Business Office, Mineralogical Society of America, 1625 I Street, N.W., Suite 414, Washington, D.C. 20006, U.S.A. Please remit $5.00 in advance for the microfiche.

TABLE 4. Positional parameters

Atom	x	y	z
Si	0.3251 (3)	0.1141 (1)	0.6540 (13)
Be1	0.1726 (2)	0.052 49 (7)	0.1562 (7)
Be2	0.3264 (2)	0.220 23 (7)	0.1509 (7)
H1	0	0.2006 (4)	0.4203 (16)
H2	0.5	0.3675 (4)	0.4530 (16)
O1	0.2899 (2)	0.1243 (1)	0
O2	0.2095 (3)	0.4030 (1)	0.5065 (6)
O3	0.2938 (2)	0.2091 (1)	0.5012 (6)
O4	0.5	0.0847 (2)	0.5916 (7)
O5	0.5	0.2553 (2)	0.0877 (8)
O6	0	0.0876 (2)	0.0978 (8)

Note: Values in parentheses represent esd's for last decimal place.

TABLE 5. Apparent vibrational parameters

Atom	U_{11}*	U_{22}*	U_{33}*	U_{12}*	U_{13}*	U_{23}*	B_{eq}**
Si	0.0103 (8)	0.0030 (8)	0.0090 (7)	−0.0008 (11)	−0.0004 (17)	0.0000 (13)	0.59 (3)
Be1	0.0104 (7)	0.0054 (5)	0.0107 (5)	0.0008 (5)	−0.0007 (9)	−0.0006 (9)	0.80 (2)
Be2	0.0126 (6)	0.0059 (9)	0.0111 (6)	0.0003 (5)	−0.0005 (9)	0.0013 (10)	0.78 (3)
H1	0.0210 (28)	0.0289 (28)	0.0351 (31)	0	0	−0.0176 (28)	2.2 (1)
H2	0.0295 (32)	0.0250 (28)	0.0407 (35)	0	0	−0.0153 (29)	2.5 (1)
O1	0.0136 (10)	0.0042 (7)	0.0096 (8)	−0.0015 (6)	0.0018 (7)	−0.0005 (6)	0.72 (3)
O2	0.0126 (10)	0.0053 (7)	0.0101 (10)	−0.0020 (6)	−0.0012 (7)	0.0003 (6)	0.74 (4)
O3	0.0153 (12)	0.0047 (6)	0.0099 (9)	0.0015 (7)	−0.006 (8)	0.0005 (6)	0.79 (4)
O4	0.0077 (10)	0.0092 (10)	0.0172 (17)	0	0	−0.0027 (10)	0.91 (6)
O5	0.0105 (12)	0.0101 (12)	0.0158 (18)	0	0	0.0028 (11)	0.96 (6)
O6	0.0122 (11)	0.0104 (12)	0.0137 (18)	0	0	0.0011 (11)	1.01 (5)

* $T = \exp[-2\pi^2(U_{11}h^2a^{*2} + U_{22}k^2b^{*2} + U_{33}l^2c^{*2} + 2U_{12}hka^*b^* + 2U_{13}hla^*c^* + 2U_{23}klb^*c^*)$.
** $B_{eq} = (8/3)\pi^2(U_{11} + U_{22} + U_{33})$.

can be precisely located. The H–O bond distances reported herein have not been "corrected" for librational motion of the H atom; however, the effect of such a correction is expected to lengthen the H–O bond distances somewhat. Figure 1 shows the positions of the hydroxyl groups viewed down the X axis. The O5 and O6 oxygens are both coordinated to 2 Be atoms and 1 H atom in essentially a triangular planar arrangement.

TABLE 6. Eigenvalues and eigenvector components of vibrational tensors

Atom	Axis	rms (Å) displacement	Angle (°) with respect to a	b	c
Si	1	0.054 (7)	83 (8)	6 (8)	90 (12)
	2	0.095 (5)	104 (57)	88 (14)	165 (57)
	3	0.102 (5)	16 (52)	96 (9)	104 (57)
Be1	1	0.073 (4)	94 (3)	8 (7)	84 (9)
	2	0.103 (3)	103 (13)	85 (9)	166 (13)
	3	0.119 (3)	13 (12)	84 (3)	102 (13)
Be2	1	0.074 (5)	93 (4)	14 (9)	103 (9)
	2	0.106 (4)	107 (30)	104 (9)	158 (25)
	3	0.113 (3)	17 (30)	91 (8)	107 (30)
H1	1	0.119 (13)	90	40 (4)	50 (4)
	2	0.145 (10)	180	90	90
	3	0.223 (9)	90	130 (4)	40 (4)
H2	1	0.125 (13)	90	31 (4)	59 (4)
	2	0.172 (9)	180	90	90
	3	0.224 (8)	90	121 (4)	31 (4)
O1	1	0.063 (5)	82 (4)	9 (3)	87 (6)
	2	0.094 (4)	69 (7)	90 (7)	159 (7)
	3	0.121 (4)	22 (7)	99 (3)	70 (7)
O2	1	0.069 (5)	76 (4)	14 (4)	90 (7)
	2	0.098 (5)	110 (11)	85 (7)	160 (11)
	3	0.116 (4)	25 (10)	103 (4)	110 (11)
O3	1	0.067 (5)	98 (3)	10 (5)	96 (6)
	2	0.100 (5)	94 (8)	97 (6)	171 (7)
	3	0.125 (5)	9 (5)	82 (3)	95 (8)
O4	1	0.089 (6)	0	90	90
	2	0.091 (6)	90	163 (6)	107 (6)
	3	0.134 (6)	90	107 (6)	17 (6)
O5	1	0.095 (7)	90	158 (8)	68 (8)
	2	0.102 (6)	180	90	90
	3	0.130 (6)	90	68 (8)	22 (8)
O6	1	0.101 (6)	90	11 (11)	101 (11)
	2	0.110 (5)	180	90	90
	3	0.126 (7)	90	79 (11)	11 (11)

Van der Waals radii for several atoms have recently been computed by Spackman (1986) using interatomic potentials based upon the Gordon-Kim-Rae (GKR) electron-gas model. Spackman has reported two radii for H that are based on different values of the exponent in the H-atom electron-density function. The average of these two radii is 1.23 Å, whereas the Van der Waals radius for O is given as 1.46 Å. The sum of the GKR Van der Waals radii of H and O is therefore 2.69 Å. If the observed H···O distance is less than the sum of the Van der Waals radii for H and O, then we may consider a H bond to have formed (Hamilton and Ibers, 1968). The H···O distances shown in Figure 1 of 2.33 and 2.39 Å are significantly less than 2.69 Å and therefore indicate weak H bonding between O5 and O6. These bonds are termed "weak" since H···O H-bonded distances can be considerably shorter (e.g., the H···O distance is approximately 1.74 Å in ice-I).

The two weak H bonds appear to be virtually linear, with the O5–H1···O6 bond being somewhat shorter than the O6–H2···O5 bond. The difference in H-bond distances is most likely determined by structural requirements of the beryllosilicate framework, although differences in the electron-density distribution about the acceptor oxygens could also be a factor. Examination of the latter possibility must await an experimental deter-

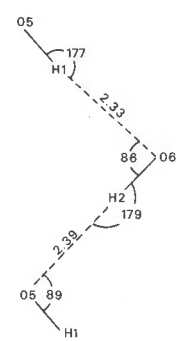

Fig. 1. Atoms involved in H bonding viewed on the (200) plane. Distances are in ångströms; angles in degrees. Dashes denote H-bond interactions.

TABLE 7. Selected interatomic distances and angles

Si tetrahedron		Be1 tetrahedron		Be2 tetrahedron	
Si–O1	1.617 (6)	Be1–O1	1.660 (2)	Be2–O1	1.649 (2)
–O2	1.626 (4)	–O2	1.638 (3)	–O3	1.634 (3)
–O3	1.633 (4)	–O2′	1.643 (2)	–O3′	1.651 (2)
–O4	1.614 (3)	–O6	1.619 (2)	–O5	1.630 (5)
Mean	1.623	Mean	1.640	Mean	1.641
O1–O2	2.667 (2)	O1–O2	2.717 (3)	O1–O3	2.681 (2)
O1–O3	2.621 (2)	O1–O2′	2.650 (2)	O1–O3′	2.645 (3)
O1–O4	2.683 (3)	O1–O6	2.626 (2)	O1–O5	2.740 (9)
O2–O3	2.640 (3)	O2–O2′	2.635 (1)	O3–O3′	2.712 (2)
O2–O4	2.638 (2)	O2–O6	2.699 (3)	O3–O5	2.701 (5)
O3–O4	2.647 (3)	O2′–O6	2.736 (3)	O3′–O5	2.646 (4)
Mean	2.649	Mean	2.677	Mean	2.679
O1–Si–O2	110.6 (2)	O1–Be1–O2	110.9 (2)	O1–Be2–O3	106.5 (1)
O1–Si–O3	107.5 (2)	O1–Be1–O2′	106.7 (1)	O1–Be2–O3′	106.5 (2)
O1–Si–O4	112.2 (3)	O1–Be1–O6	106.4 (2)	O1–Be2–O5	113.4 (4)
O2–Si–O3	108.2 (3)	O2–Be1–O2′	106.9 (1)	O3–Be2–O3′	111.3 (1)
O2–Si–O4	109.0 (2)	O2–Be1–O6	111.9 (2)	O3–Be2–O5	111.6 (2)
O3–Si–O4	109.2 (2)	O2′–Be1–O6	114.0 (2)	O3′–Be2–O5	107.5 (4)
Mean	109.5	Mean	109.5	Mean	109.5
O1 triangle		O2 triangle		O3 triangle	
O1–Be1	1.660 (2)	O2–Be1	1.638 (3)	O3–Be2	1.634 (3)
–Be2	1.649 (2)	–Be1′	1.643 (2)	–Be2′	1.651 (3)
–Si	1.617 (6)	–Si	1.626 (4)	–Si	1.633 (4)
Mean	1.642	Mean	1.636	Mean	1.640
Be1–O1–Be2	121.7 (1)	Si–O2–Be1	117.9 (2)	Si–O3–Be2	118.8 (2)
Be1–O1–Si	118.2 (1)	Si–O2–Be1′	122.7 (2)	Si–O3–Be2′	120.6 (2)
Be2–O1–Si	117.2 (2)	Be1–O2–Be1′	116.5 (1)	Be2–O3–Be2′	116.6 (1)
Mean	119.0	Mean	119.0	Mean	118.7
O4 atom		O5 triangle		O6 triangle	
O4–Si	1.614 (3)	O5–Be2	1.631 (5)	O6–Be1	1.619 (2)
–Si	1.614 (3)	–Be2	1.631 (5)	–Be1	1.619 (2)
Mean	1.614	–H1	0.952 (11)	–H2	0.952 (7)
		Be2–O5–Be2	136.2 (7)	Be1–O6–Be1	136.6 (2)
		Be2–O5–H1	110.9 (3)	Be1–O6–H2	110.7 (1)
		Be2–O5–H1	110.9 (3)	Be1–O6–H2	110.7 (1)
Si–O4–Si	141.6 (3)	Mean	119.4	Mean	119.3

mination of the electron-density distribution and electrostatic potential of bertrandite.

ACKNOWLEDGMENTS

We thank Carl Francis of the Harvard University Mineralogical Museum for providing the bertrandite crystal (HMM no. 103454). J.W.D. wishes to recognize support from the University of Missouri Research Reactor Facility and NSF Grant EAR-77-23114 to G. V. Gibbs and P. H. Ribbe during the period of data collection. J.W.D. also thanks R. M. Hazen and L. W. Finger for assistance in profile analysis while J.W.D. was visiting the Geophysical Laboratory of the Carnegie Institution of Washington.

REFERENCES

Bacon, G.E. (1975) Neutron diffraction (third edition). Oxford University Press, Oxford, England.

Becker, P. (1977) The theoretical models of extinction. Their domain of applicability. Acta Crystallographica, A33, 243–249.

Becker, P.J., and Coppens, P. (1974a) Extinction within the limit of the Darwin transfer equations. I. General formalisms for primary and secondary extinction and their application to spherical crystals. Acta Crystallographica, A30, 129–147.

——— (1974b) Extinction within the limit of the Darwin transfer equations. II. Refinement of extinction in spherical crystals of SrF_2 and LiF. Acta Crystallographica, A30, 148–153.

——— (1975) Extinction within the limit of the Darwin transfer equations. III. Non-spherical crystals and anisotropy of extinction. Acta Crystallographica, A31, 417–425.

Busing, W.R., Martin, K.O., and Levy, H.A. (1962) ORFLS, a FORTRAN least-squares refinement program. U.S. National Technical Information Service, ORNL-TM-305.

Coppens, P. (1975) Program LINEX. Chemistry Department, State University of New York at Buffalo, Acheson Hall, Buffalo, NY 14214.

Coppens, P., and Hamilton, W.C. (1970) Anisotropic extinction corrections in the Zachariasen approximation. Acta Crystallographica, A26, 71–83.

Downs, J.W., and Gibbs, G.V. (1981) The role of the BeOSi bond in the structures of beryllosilicate minerals. American Mineralogist, 66, 819–826.

Downs, J.W., Ross, F.K., and Gibbs, G.V. (1985) The effects of extinction on the refined structural parameters of crystalline BeO: A neutron and γ-ray diffraction study. Acta Crystallographica, B41, 425–431.

Hamilton, W.C. (1965) Significance tests on the crystallographic *R* factor. Acta Crystallographica, 18, 502–510.

Hamilton, W.C., and Ibers, J.A. (1968) Hydrogen bonding in solids. W.A. Benjamin, Inc., New York.

Hazen, R.M., and Au, A.Y. (1986) High-pressure crystal chemistry of phenakite (Be_2SiO_4) and bertrandite [$Be_4Si_2O_7(OH)_2$]. Physics and Chemistry of Minerals, 13, 69–78.

Koester, L. (1977) Neutron scattering lengths and fundamental neutron interactions. In G. Hohler, Ed., Neutron physics, Springer tracts in modern physics, vol. 80. Springer-Verlag, New York.

Lehmann, M.S., and Larsen, F.K. (1974) A method for location of the

peaks in step-scan–measured Bragg reflexions. Acta Crystallographica, A30, 580–584.

Petkof, B. (1976) Beryllium. In Mineral facts and problems, 1975 edition. U.S. Bureau of Mines Bulletin, 667, 137–146.

Solov'eva, L.P., and Belov, N.V. (1965) Precise determination of the crystal structure of bertrandite, $Be_4[Si_2O_7](OH)_2$. Soviet Physics Crystallography, 9, 458–460.

Spackman, M.A. (1986) Atom-atom potentials via electron gas theory. Journal of Chemical Physics, 85, 6579-6586.

Thornley, F.R., and Nelmes, R.J. (1974) Highly anisotropic extinction. Acta Crystallographica, A30, 748–757.

Manuscript received February 19, 1987
Manuscript accepted May 29, 1987